Current Optics and Photonics
Vol. 2, No. 5, October 2018, pp. 474-481

ISSN: 2508-7266(Print) / ISSN: 2508-7274(Online)
DOI: https://doi.org/10.3807/COPP.2018.2.5.474

Polarization Phase-shifting Technique for the Determination of a Transparent Thin Film's Thickness Using a Modified Sagnac Interferometer

Rapeepan Kaewon[1], Chutchai Pawong[2], Ratchapak Chitaree[3], and Apichai Bhatranand[1]*

[1]*King Mongkut's University of Technology Thonburi, Faculty of Engineering, Department of Electronic and Telecommunication Engineering, Bangkok 10140, Thailand*
[2]*Rajamangala University of Technology Krungthep, Faculty of Science and Technology, Physics Division, Bangkok 10120, Thailand*
[3]*Mahidol University, Faculty of Science, Department of Physics, Bangkok 10400, Thailand*

(Received June 22, 2018 : revised August 1, 2018 : accepted August 8, 2018)

We propose a polarization phase-shifting technique to investigate the thickness of Ta_2O_5 thin films deposited on BK7 substrates, using a modified Sagnac interferometer. Incident light is split by a polarizing beam splitter into two orthogonal linearly polarized beams traveling in opposite directions, and a quarter-wave plate is inserted into the common path to create an unbalanced phase condition. The linearly polarized light beams are transformed into two circularly polarized beams by transmission through a quarter-wave plate placed at the output of the interferometer. The proposed setup, therefore, yields rotating polarized light that can be used to extract a relative phase via the self-reference system. A thin-film sample inserted into the cyclic path modifies the output signal, in terms of the phase retardation. This technique utilizes three phase-shifted intensities to evaluate the phase retardation via simple signal processing, without manual adjustment of the output polarizer, which subsequently allows the thin film's thickness to be determined. Experimental results show that the thicknesses obtained from the proposed setup are in good agreement with those acquired by a field-emission scanning electron microscope and a spectroscopic ellipsometer. Thus, the proposed interferometric arrangement can be utilized reliably for non-contact thickness measurements of transparent thin films and characterization of optical devices.

Keywords : Polarization phase-shifting technique, Sagnac interferometer, Rotating polarized light, Thin-film thickness measurement, Transparent thin films
OCIS codes : (230.4040) Mirrors; (230.5160) Photodetectors; (260.5430) Polarization

I. INTRODUCTION

The use of polarized light as a probe for nondestructive measurement in phase-shifting interferometry, to investigate the properties of optical samples, is attracting considerable attention [1-4]. The phase shifting of the polarized light typically employs rotating polarized light (RPL), because it offers certain advantages over conventional polarized light, in terms of polarization controllability and measurement speed [5]. The RPL can theoretically be generated by combining two orthogonal circularly polarized beams, with their phase difference controlled by a transducer. This combination can be achieved by utilizing an interferometric configuration, whereby two optical beams interfere with each other to form an output beam [6, 7]. Normally the transducer for phase modulation is a piezoelectric transducer (PZT), whose operation is driven by a periodic signal. This can be considered a dynamic phase-shifting scheme. Numerous phase-shifting interferometric arrangements, such as the Michelson and Mach-Zehnder configurations, were proposed for generating RPL [5, 8-10]. Although the RPL outputs from such configurations are satisfactory, the optical hardware configurations used in the abovementioned studies are very different. Even so, each scheme involves a large

*Corresponding author: apichai.bha@mail.kmutt.ac.th, ORCID 0000-0002-3468-918X
Color versions of one or more of the figures in this paper are available online.

number of components and has complex setup procedures. With this background, a recent work proposed an alternative scheme for phase-shifting interferometry based on a configuration known as the cyclic-path interferometer [11-13]. In this scheme, the generation method is robust to external environments and vibrational disturbances [14].

The present study investigates the potential of the RPL generated by our modified Sagnac interferometer (so called "mSI") as a probe for nondestructive thickness measurements of Ta_2O_5 thin films deposited on a BK7 substrate. The phase retardation resulting from the presence of the thin-film sample in the optical path of our system can be extracted directly from the unbalanced RPL output beam, using a simple signal algorithm. We also demonstrate that our proposed mSI has an edge over previously utilized interferometric systems [15-20], because of its compact arrangement and simple method for thickness determination. Thus far the control of phase shifting in a polarization phase shifter has mainly involved the manual rotation of wave retarders, which is a fairly complicated procedure [13, 21]. Hence, we apply herein an alternative "automatic" scheme for phase-shifting interferometry using a PZT. The use of polarization phase shifting (obviating the need to rotate the polarizer), which has never been done in previous interferometric systems, is significant. We use the intercept points of the output intensities of three recorded and analyzed sample signals with respect to the initial self-reference signal. In the final stage of this study, we compare the experimental results to the corresponding measured values obtained using commercial equipment, to evaluate the mSI's performance.

II. METHODS

2.1. Operation of the mSI System Without a Sample

Figure 1 shows the schematic of the mSI system. A light source (LS) emits a beam of linearly polarized light, with a polarization that can be tuned by a half-wave plate (HW) oriented at 22.5° with respect to the axis of the polarizing beam splitter (PBS). Hence, the Jones vector E_i representing the electric field of the linearly polarized light beam exiting the HW is given as follows:

$$E_i = \frac{1}{\sqrt{2}}\begin{bmatrix}1\\1\end{bmatrix} \tag{1}$$

The PBS splits the polarized light into two orthogonal linearly polarized beams traveling in perpendicular directions (*i.e.* transmitted and reflected light beams). On the one hand, the transmitted light beam with electric field E_{iT} traveling along path 1 (PBS→M1→WP→PZT(M2)→PBS→QW) is linearly parallel to the plane of the interferometer, when no sample is inserted. On the other hand, the reflected light beam with electric field E_{iR} propagating along path 2

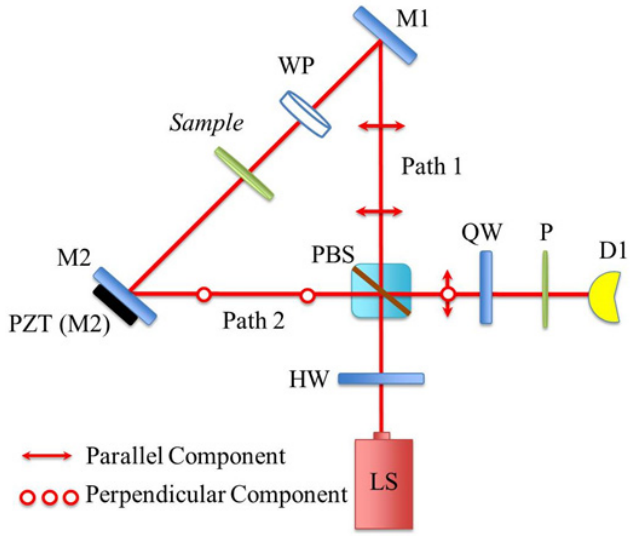

FIG. 1. Schematic of the modified Sagnac interferometer (mSI).

(PBS→PZT(M2)→WP→M1→PBS→QW) is linearly perpendicular to the plane of the interferometer. The vibrating mirror is driven by the PZT, and the phase introduced by the mirror changes with time. Basically, both light beams in the common path experience an equal "vibration" with balanced phase. A general wave plate (WP) is positioned between mirrors M1 and M2 and affixed to a PZT (PZT(M2)), to generate a phase shift via its fast and slow axes. The WP creates unbalanced phase, that is, a relative phase change between the orthogonal polarization components of the light traveling through the system. Therefore, the Jones vector representing the light signals E_{iT} and E_{iR} can be written as follows:

$$E_{iT} = Q \cdot T_{PBST} \cdot M \cdot W \cdot M \cdot T_{PBST} \cdot E_i = \frac{1}{2}\begin{bmatrix}\exp(i\delta_f)\\ -i\exp(i\delta_f)\end{bmatrix} \tag{2}$$

$$E_{iR} = Q \cdot T_{PBSR} \cdot M \cdot W \cdot M \cdot T_{PBSR} \cdot E_i = \frac{1}{2}\begin{bmatrix}-i\exp[i(\delta_s+\delta_{M2}(t)+\delta_{M1})]\\ \exp[i(\delta_s+\delta_{M2}(t)+\delta_{M1})]\end{bmatrix} \tag{3}$$

where T_{PBST} and T_{PBSR} represent the Jones matrices of the linear PBS, following a previous study [5]. The phases of the light beams δ after the deflection of mirrors from M1 and PZT(M2) are δ_{M1} and $\delta_{M2}(t)$, respectively. $\delta_{M2}(t)$ represents the time-dependent phase shift. The Jones notations for each mirror are given as follows:

$$M = \begin{bmatrix}1 & 0\\ 0 & \exp(i\delta)\end{bmatrix} \tag{4}$$

The Jones matrix W of a linear birefringent WP, described in terms of a Jones matrix in which δ_f and δ_s are phase

retardances introduced by the fast and slow eigenmodes, can be expressed as [22]:

$$W = \begin{bmatrix} \exp(i\delta_f) & 0 \\ 0 & \exp(i\delta_s) \end{bmatrix} \tag{5}$$

Q denotes the Jones matrix for the output quarter-wave plate (QW), oriented with optical axes at -45° with respect to the transmission axis of the PBS, can be expressed as:

$$Q = \frac{1}{\sqrt{2}} \begin{bmatrix} 1 & -i \\ -i & 1 \end{bmatrix} \tag{6}$$

These two beams then recombine at the PBS, and are subsequently transformed into two circularly polarized light beams by QW. The resulting beam becomes a rotating polarized light beam, called the RPL. Therefore, the Jones vector representing the electric field of the output light exiting QW can be expressed as follows:

$$\begin{aligned} E_{iT} + E_{iR} &= \frac{1}{2}\left\{ \begin{bmatrix} 1 \\ -i \end{bmatrix} \exp(i\delta_f) + \begin{bmatrix} 1 \\ i \end{bmatrix} \exp[i(\delta_s + \delta_{M2}(t) + \delta_{M1} - \frac{\pi}{2})] \right\} \\ &= \begin{bmatrix} \sin(\delta_t(t)) \\ \cos(\delta_t(t)) \end{bmatrix} \exp\left[i\left(\frac{\delta_f}{2} + \frac{\delta_s}{2} + \frac{\delta_{M2}(t)}{2} + \frac{\delta_{M1}}{2} - \frac{\pi}{4} \right) \right] \end{aligned} \tag{7}$$

where $\delta_t(t) = \delta_{M2}(t) + \delta_s + \delta_{M1} - \delta_f$. The time-varying phase suggests that the RPL's orientation depends on the mirror's vibration. Subsequently the output light after QW enters the linear polarizer (P) and the photodetector (D1). The rotation of the linearly polarized output beam with respect to a static linear polarizer automatically allows the orientation of the beam, caused by the initial phase from the apparatus, to be offset. This action is marked by a time called the offset time, which indicates a new starting time for a subsequently introduced phase shift. Therefore, any phase shift introduced later by a thin-film sample is measured relative to the offset time.

2.2. Operational Procedure for the mSI System with an Inserted Sample

In this study, we utilized the initial interference RPL generated by the mSI as a measuring tool to determine the phase shift introduced by an inserted thin-film sample. The sample was positioned between M1 and PZT(M2), as shown in Fig. 1. The two beams travel along path 1 corresponding to $E_{iT,Sample}$ (PBS→M1→WP→*Sample*→PZT(M2)→PBS→QW) and path 2 corresponding to $E_{iR,Sample}$ (PBS→PZT(M2)→ *Sample*→WP→M1→PBS→QW). The Jones matrix S of the homogenous sample is expressed as follows [5]:

$$S = \begin{bmatrix} T_a & 0 \\ 0 & T_b \exp(i\Delta) \end{bmatrix} \tag{8}$$

where T_a and T_b represent the transmission coefficients along the principal axes of the transparent sample, and Δ is the phase retardation introduced by the sample. The Jones vector representing the summation of the electric fields of the transmitted and reflected light beams traveling through the PBS can be expressed as follows:

$$\begin{aligned} &E_{iT,Sample} + E_{iR,Sample} \\ &= \frac{1}{2}\left\{ \begin{bmatrix} T_a \exp(i\delta_f) \\ -iT_a \exp(i\delta_f) \end{bmatrix} + \begin{bmatrix} -iT_b \exp[i(\Delta + \delta_s + \delta_{M2}(t) + \delta_{M1})] \\ T_b \exp[i(\Delta + \delta_s + \delta_{M2}(t) + \delta_{M1})] \end{bmatrix} \right\} \end{aligned} \tag{9}$$

Furthermore, the Jones vector $E^{\theta}_{out,polarizer}$ of the output beam emerging from the mSI setup and passing through the polarizer can be rewritten as:

$$E^{\theta}_{out,polarizer} = P(\theta)\left[E_{iT,Sample} + E_{iR,Sample} \right] \tag{10}$$

where P(θ), representing the Jones matrix of the linear polarizer (P), can be expressed as $\begin{bmatrix} \cos^2\theta & \cos\theta\sin\theta \\ \cos\theta\sin\theta & \sin^2\theta \end{bmatrix}$ [3]. The transmission axis of P is aligned at an angle θ with respect to the reference axis. In this study, the output polarizer is fixed at 45° with respect to the reference axis throughout the investigation. Normally phase shifting can be accomplished by adjusting the axis orientation of the output polarizer and collecting the output intensities at desired angles. For our proposed scheme, the QW placed at the output arm transforms the output light to RPL. The orientation of the RPL is time-varying with respect to the transmission axis of the polarizer. This RPL is automatically rotated with the orientation of the polarizer's transmission axis kept fixed. Here we note that the variation of required intensities is obtained by the phase modulation, not by adjusting the polarizer. Thus the time-varying orientation of RPL allows convenient acquisition of the output light intensities at 0°, 45°, and 90°. Thus, from Eq. (10) and the expression of $I^{\theta}_{out,polarizer} = E^{\theta}_{out,polarizer} * E^{\theta *}_{out,polarizer}$, the mentioned intensities can be found as

$$I^{0^\circ}_{out,polarizer} = \frac{T_a^2}{4} + \frac{T_a T_b}{2}\sin(\Delta + \delta_t(t)) + \frac{T_b^2}{4}, \tag{11}$$

$$I^{45^\circ}_{out,polarizer} = \frac{T_a^2}{4} + \frac{T_a T_b}{2}\cos(\Delta + \delta_t(t)) + \frac{T_b^2}{4}, \tag{12}$$

$$I^{90^\circ}_{out,polarizer} = \frac{T_a^2}{4} - \frac{T_a T_b}{2}\sin(\Delta + \delta_t(t)) + \frac{T_b^2}{4}. \tag{13}$$

The phase retardation $\Delta+\delta_t$ (t), introduced by an inserted Ta_2O_5 thin-film sample, can be resolved from Eqs. (11) to (13) as

$$\Delta+\delta_t(t) = \tan^{-1}\left[\frac{I^{0^\circ}_{\text{out,polarizer}} - I^{90^\circ}_{\text{out,polarizer}}}{2I^{45^\circ}_{\text{out,polarizer}} - I^{90^\circ}_{\text{out,polarizer}} - I^{0^\circ}_{\text{out,polarizer}}}\right]. \quad (14)$$

As mentioned in Section 2.1, the offset time is already identified and designates a new initial time for any phase retardation due to further perturbation. In this case, the self-reference technique mentioned in Section 3 is employed to determine the phase shift introduced by a thin-film sample. Since the measurements of corresponding intensities are always done relative to a new starting time (offset time), the time-varying phase δ(t) in Eq. (14) can be canceled out. Finally, the phase-shift introduced by a thin-film sample can be expressed as:

$$\Delta = \arctan\left[\frac{I^{0^\circ}_{\text{out,polarizer}} - I^{90^\circ}_{\text{out,polarizer}}}{2I^{45^\circ}_{\text{out,polarizer}} - I^{90^\circ}_{\text{out,polarizer}} - I^{0^\circ}_{\text{out,polarizer}}}\right]. \quad (15)$$

where $I^{0^\circ}_{\text{out,polarizer}}$, $I^{45^\circ}_{\text{out,polarizer}}$, and $I^{90^\circ}_{\text{out,polarizer}}$ are measurable from the setup. Hence the phase retardation introduced by the optical sample can consequently be estimated by the method described in the next section.

2.3. Determination of the Transparent Sample's Thickness

The transmittance T of an output light signal under various conditions must be carefully evaluated [23]. The phase retardation Δ can be expressed as $4\pi n_1 d/\lambda$, where n_1 denotes the refractive index of the deposited film (2.136 for Ta_2O_5), d is the film's thickness, and λ is the light's wavelength (632.8 nm). The phase retardation Δ obtained from Eq. (15) is in an arctan function form that periodically repeats every 180° (π radians). Therefore, the phase shift Δ can be written in terms of the order number m as $\Delta_m = \Delta + m\pi$. The phase shift Δ can also be "accumulated" (or increased) to match the measured Δ value by adding integer multiples of π, represented as $m\pi$, where m denotes the cumulative integer chosen as the sign changes from negative to positive (*i.e.* it specifies the number of periods of the arctan function of Δ). This relation must be satisfied prior to calculating the thickness d, to determine the exact order of the periodic arctan function of Δ [18]. The parameter d_{cutoff} is employed to determine the appropriate value of the order number m when the deposition time t_d and approximate deposition rate R_d are known. In this study, R_d from the commercial UHV sputtering system (AJA International Inc., ATC 2000-F) used is 15 nm/min. The cutoff thickness d_{cutoff}, at the point at which the second cycle begins ($\Delta_S = \pi$), can be expressed as $\lambda/4n_1$. Accordingly, the appropriate value of m can be determined using $t_d R_d/d_{\text{cutoff}}$. For Ta_2O_5 with a refractive index of 2.136, and a red laser having a wavelength of 632.8 nm, d_{cutoff} is found to be 70 nm. According to this information, the values of m at 10, 15, and 20 min with rate $R_d = 15$ nm/min are 2, 4, and 6 respectively. Eventually the thin-film thickness d_1 can be determined with an appropriate value of m as:

$$d = \frac{\Delta_m \lambda}{4\pi n_1} \quad (16)$$

III. SIGNAL PROCESSING ALGORITHM TO EVALUATE PHASE RETARDATION

A signal algorithm to evaluate the phase shift was employed to track the three output intensities mentioned in Eq. (15). A digital oscilloscope (Yokogawa, model DL1620) was used to acquire the desired data, with optimized amplitude and frequency settings of a modulating sinusoidal trigger signal set at 1.8 V and 48 Hz respectively. Our proposed setup did not have a reference arm; hence, the outer trigger function from the oscilloscope was required to get an output waveform for the self-reference signal prior to sample insertion. The standard statistical cross correlation was checked, with the positions corresponding to the first to third calibrations (of the self-reference signal) corresponding to the three intensities before sample insertion. Figure 2 shows the signal intensities obtained with and without the sample. In both cases, the linear polarizer before the recording plane was not rotated. The amplitude and phase information were fixed in the cyclic path without the sample, because the polarizer was oriented at 45° with respect to the PBS axis. A WP was set as a quarter-wave plate to introduce the prior phase shift. Afterward, upon inserting a sample into the interferometer stage between M1 and PZT(M2), the output light intensity was normally perturbed in terms of its amplitude and phase. This intensity perturbation was the key for tracking the differential amplitudes and phase before and after sample insertion. The RPL was generated from the mSI, whereas the polarizer positioned behind QW yielded a self-reference signal, with intensities corresponding to θ relative to the reference. We refer to this output as $I^{\theta}_{\text{out,polarizer}}$. The RPL orientation was referred to as θ, and the output light intensity emerging from "P(45°)" was fixed. Subsequently, the specific changes in the intensities arising from the introduction of the sample could be clearly observed when the polarizer was set at 45° with respect to the PBS axis. The output light intensities $I^{0^\circ}_{\text{out,polarizer}}$, $I^{45^\circ}_{\text{out,polarizer}}$, and $I^{90^\circ}_{\text{out,polarizer}}$ indicated in the waveforms depicted in Figs. 2(a)~2(c), respectively, were substituted into Eq. (15) to calculate the phase retardation Δ, which can be translated to the film thickness using Eq. (16). It should be noted that *all required intensities were obtained with no moving parts involved in the polarizing devices*. This is obviously due to the time-dependent orientation of the RPL.

As previously mentioned, our proposed technique uses a self-reference signal prior to the introduction of the thin-film sample. The influence of glass (BK7) thickness is

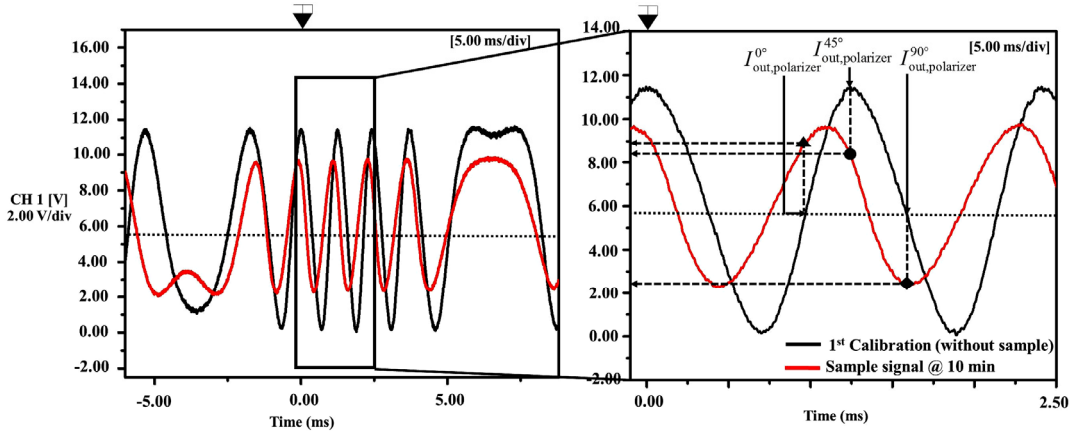

(a)

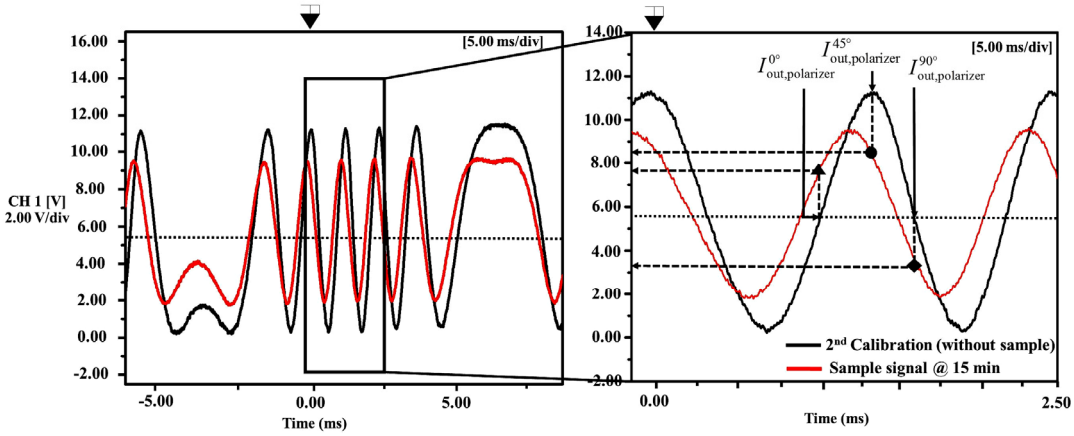

(b)

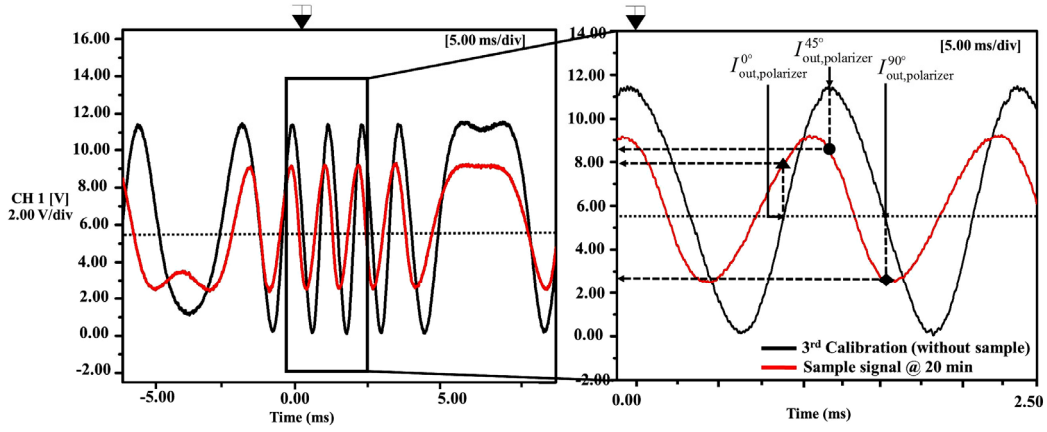

(c)

FIG. 2. Comparison of the relative phases of output signals with and without an inserted sample, for various deposition times of (a) 10 min, (b) 15 min, and (c) 20 min.

also investigated, and the results show that the recorded output intensities with and without pure glass placed in our mSI system are almost identical. The phase shift caused by the glass alone is only 0.0073 rad, which is considered insignificant and can be neglected. The BK7 substrate used in this work is 0.94 mm thick. Hence, our proposed scheme is suitable for a glass sample of thickness less than 1 mm.

IV. EXPERIMENTAL RESULTS AND DISCUSSION

Transparent Ta_2O_5 thin-films were deposited via pulsed dc reactive magnetron sputtering from a 2″-diameter tantalum (Ta: 99.995%) target, using a commercial UHV sputtering system (AJA International, Inc. ATC 2000-F). The film

thicknesses obtained by our mSI setup were compared to those acquired via two conventional techniques: variable-angle spectroscopic ellipsometry (VASE; J.A. Woollam) and field-emission scanning electron microscopy (FE-SEM).

4.1. Ta_2O_5 Thin Film Measurement

The Ta_2O_5 thin-film samples of different thicknesses deposited on the BK7 substrates were characterized by the mSI setup. The sample was inserted into the light beam's path between PZT(M2) and M1. The output light intensities detected by D1 in terms of voltages were processed by a program at the different intensity points indicated in Fig. 2. The data required to solve Eqs. (15) and (16) could be determined by applying the signal algorithm discussed in Section 3. The three output light intensities listed in Table 1 are the average maximum intensities obtained from Figs. 2(a)~2(c) for the unchanged polarizer orientation and given deposition times.

TABLE 1. Output light intensities as detected by the unchanged polarizer orientation under study conditions

Sample	Average maximum intensity (volts)		
	$I^{0°}_{\text{out,polarizer}}$	$I^{45°}_{\text{out,polarizer}}$	$I^{90°}_{\text{out,polarizer}}$
$Ta_2O_5 \equiv 10$ min	8.95	8.46	2.42
$Ta_2O_5 \equiv 15$ min	7.72	8.52	3.24
$Ta_2O_5 \equiv 20$ min	7.98	8.50	2.73

These intensities were used as numerical data for Eq. (15) to determine the phase retardation for each deposition time. From the graphs shown in Figs. 2(a)~2(c), we calculated the phase retardations with the inserted sample for deposition times of 10, 15, and 20 min to be 0.87, 0.64, and 0.70 rad respectively. The maximum and minimum T values must be carefully tracked, along with the phase retardation, to determine the appropriate m value. The film thickness can eventually be determined using Eq. (16) (*e.g.* $d(10\text{ min}) = (0.87 + 2\pi) \times \lambda/4\pi n_1 = 168.6$ nm). The measured thicknesses using our proposed mSI system for deposition times of 10, 15, and 20 min were 168.6, 237.3, and 312.8 nm respectively.

4.2. VASE and FE-SEM Techniques

From the measured spectroscopic ellipsometry (SE) data, we constructed a physical model to describe the possible Ta_2O_5 film structures. For the PVD fabrication process that yields "islands" of films, the physical model was assumed to be a double-layer structure, with a Ta_2O_5-dense layer and a top surface-roughness layer, as in Fig. 3(a). We chose the proposed physical structure also because it suitably reflects the inhomogeneity of a mixture of dense material and voids for the case of island-film growth [24, 25]. This physical model was then utilized in combination with an

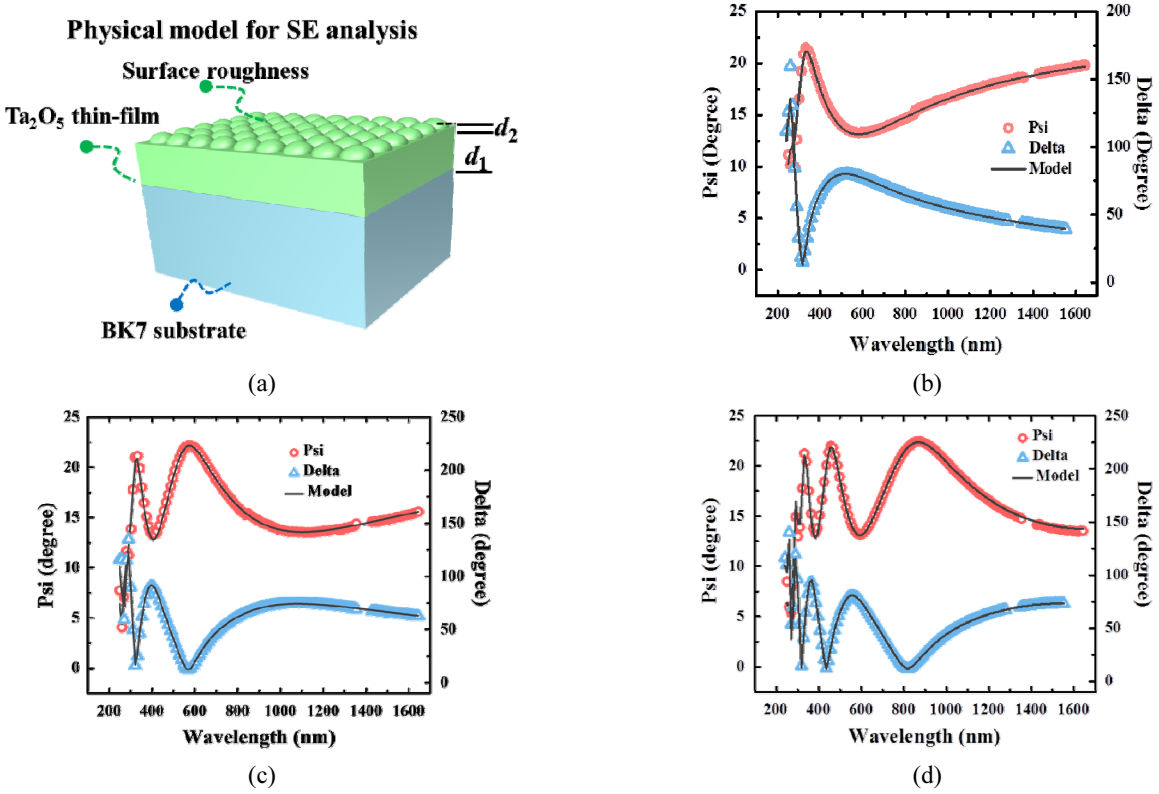

FIG. 3. Physical model proposed in this study: (a) Ta_2O_5 film structure for spectroscopic ellipsometry (SE) analysis, and Tauc-Lorentz oscillator [25] fitting curves of the ellipsometric parameters Ψ and Δ, for deposition times of (b) 10 min, (c) 15 min, and (d) 20 min.

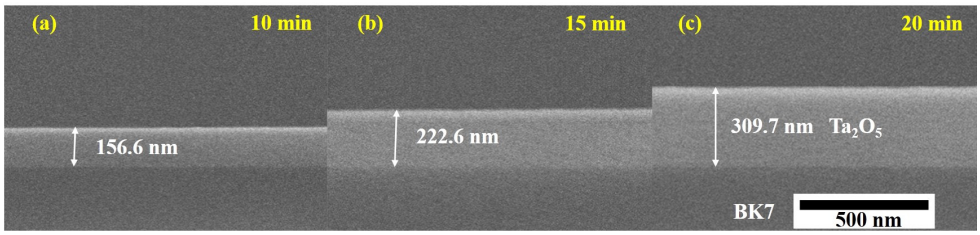

FIG. 4. Cross-sectional field-emission scanning electron microscopy (FE-SEM) images of Ta_2O_5 thin films on BK7 substrate, for deposition times of (a) 10 min, (b) 15 min, and (c) 20 min.

optical model, the Tauc-Lorentz model, to represent the optical dispersion of the Ta_2O_5 thin film [25]. Figures 3(b)~3(d) show the curves of the ellipsometric parameters ψ and Δ, fitted with the proposed film structure and the optical dispersion of the sputtered Ta_2O_5 thin films, for various deposition times. The results show that the measured data suitably agree with the predictions of the proposed inhomogeneous physical model. From the ellipsometric results, the total film thickness of the prepared sample could be determined for each corresponding deposition time. The thicknesses of the dense layer and surface roughness were summed to obtain composite thickness values of 154.2, 239.6, and 313.9 nm for deposition times of 10, 15, and 20 min respectively.

These results were further confirmed by means of cross-sectional FE-SEM micrographs (Fig. 4) of the Ta_2O_5 thin films on a BK7 substrate, for various deposition times. The films were compact, homogeneous, and perfectly adherent to the BK7 substrate. The average thicknesses obtained from image analysis of the sample cross sections for deposition times of 10, 15, and 20 min were 156.6, 222.6, and 309.7 nm respectively.

4.3. Result Comparison and Discussion

The film thickness measurements achieved with mSI, SE, and FE-SEM were compared. The differences in thickness readings between the mSI and SE and mSI and FE-SEM are 8.54% and 7.11%, 0.97% and 6.19%, and 6.19% and 0.99% for deposition times of 10, 15, and 20 min respectively. The longer the deposition time, the lower was the error. This could be explained by the deposition rate being unsteady at the beginning and becoming more linear as time went on. Nevertheless, the results were not significantly different among the SE, FE-SEM, and our proposed method. In conclusion, our approach afforded a simple setup that generates RPL, with which we can perform precise and accurate thickness measurements of thin films.

V. CONCLUSION

In this study we generated rotating polarized light (RPL) with a simple mSI setup to measure thin-film thickness. More importantly, our study successfully demonstrated the precision of the mSI method in measuring the thicknesses of Ta_2O_5 thin films deposited on a BK7 substrate, for several different deposition times. The Ta_2O_5 thin films were prepared via magnetron sputtering. The films exhibited a low absorption at high deposition rates over deposition times of 10, 15, and 20 min. The experimental results obtained with our mSI system were compared to those obtained with standard VASE and FE-SEM techniques, to verify the performance of the proposed scheme. Consequently, no significant difference was found among the three sets of results. Using our approach, generating suitable RPL, accurately determining a thin film's thickness, and characterizing the phase retardation of an optical device (*e.g.* polarizer, HWP, QWP, or liquid-crystal variable wave retarder) are possible.

ACKNOWLEDGMENT

The authors would like to acknowledge the financial support of the Thai Government Science and Technology Scholarship by way of a studentship. The authors would also like to thank Dr. Mati Horprathum for his time and advice, providing film samples, and performing film measurements.

REFERENCES

1. V. H. Flores Muñoz, N.-I. T. Arellano, D. I. Serrano García, A. Martínez García, G. Rodríguez Zurita, and L. García Lechuga, "Measurement of mean thickness of transparent samples using simultaneous phase shifting interferometry with four interferograms," Appl. Opt. **55**, 4047-4051 (2016).
2. R.-S. Chang, Z.-Y. Peng, D.-F. Chen, and C.-Y. Han, "Parallel polarization phase-shifting interferometry with a multi-loop Sagnac configuration," Optik **127**, 10122-10126 (2016).
3. S. Sarkar and K. Bhattacharya, "Polarization phase shifting cyclic interferometer for surface profilometry of non-birefringent phase samples," J. Mod. Opt. **60**, 185-189 (2013).
4. R. P. Shukla, D. V. Udupa, N. C. Das, and M. V. Mantravadi, "Non-destructive thickness measurement of dichromated gelatin films deposited on glass plates," Opt. Laser Technol. **38**, 552-557 (2006).
5. C. Pawong, R. Chitaree, and C. Soankwan, "The rotating linearly polarized light from a polarizing Mach-Zehnder

interferometer: Production and applications," Opt. Laser Technol. **43**, 461-468 (2011).
6. G. E. Sommargren, "Up/down frequency shifter for optical heterodyne interferometry," J. Opt. Soc. Am. **65**, 960-961 (1975).
7. J. Shamir and Y. Fainman, "Rotating linearly polarized light source," Appl. Opt. **21**, 364-365 (1982).
8. D. A. Jackson, A. D. Kersey, P. A. Leilabady, and J. D. C. Jones, "High frequency non-mechanical optical linear polarisation state rotator," J. Phys. E **19**, 146-148 (1986).
9. C. Pawong, R. Chitaree, and C. Soankwan, "Investigation of the use of rotating linearly polarized light for characterizing SiO2 thin film on Si substrate," in *Proc. IEEE Asia Communications and Photonics* (China, Nov. 2011), 83081I (2011).
10. R. M. A. Azzam, "Polarization Michelson interferometer as a global polarization state generator and for measurement of the coherence and spectral properties of quasimonochromatic light," Rev. Sci. Instrum. **64**, 2834-2837 (1993).
11. S. Chakraborty and K. Bhattacharya, "Real-time edge detection by cyclic-path polarization interferometer," Appl. Opt. **53**, 727-730 (2014).
12. V. H. Flores Muñoz, N. I. Toto-Arellano, B. López-Ortiz, A. Martínez García, and G. Rodríguez-Zurita, "Measurement of red blood cell characteristic using parallel phase shifting interferometry," Opt. - Int. J. Light Electron. Opt. **126**, 5307-5309 (2015).
13. B. Bhaduri, "Cyclic-path digital speckle shear pattern interferometer: use of polarization phase-shifting method," Opt. Eng. **45**, 105604-1-105604-6 (2006).
14. X. Liu, Y. Gao, and M. Chang, "A new lateral shearing interferometer for precision surface measurement," Opt. Lasers Eng. **47**, 926-934 (2009).
15. L. R. Watkins, "Automatic null ellipsometry with an interferometer," Appl. Opt. **48**, 6277-6280 (2009).
16. L. R. Watkins, "Interferometric ellipsometer," Appl. Opt. **47**, 2998-3001 (2008).
17. F.-W. Sheu and S.-Y. Liu, "Using a Mach-Zehnder interferometer to measure the phase retardations of wave plates," in *Proc. Education and Training in Optics and Photonics*, EMB1 (2007).
18. C. Zhao, J. Tan, J. Tang, T. Liu, and J. Liu, "Confocal simultaneous phase-shifting interferometry," Appl. Opt. **50**, 655-661 (2011).
19. K. Bhattacharya, "Generation of phase-modulated periodic optical signals by use of a polarization interferometer," Appl. Opt. **40**, 261-267 (2001).
20. S. Sarkar, N. Ghosh, S. Chakraborty, and K. Bhattacharya, "Self-referenced rectangular path cyclic interferometer with polarization phase shifting," Appl. Opt. **51**, 126-132 (2012).
21. L. Wang, L. Liu, Z. Luan, J. Sun, and Y. Zhou, "Polarization phase-shifting Jamin shearing interferometer," Opt. - Int. J. Light Electron. Opt. **121**, 358-361 (2010).
22. R. P. Tatam, J. D. C. Jones, and D. A. Jackson, "Optical polarisation state control schemes using fibre optics or Bragg cells," J. Phys. E **19**, 711-717 (1986).
23. J. C. Manifacier, J. Gasiot, and J. P. Fillard, "A simple method for the determination of the optical constants n, k and the thickness of a weakly absorbing thin film," J. Phys. E **9**, 1002-1004 (1976).
24. M. Horprathum, P. Chindaudom, P. Limnonthakul, P. Eiamchai, N. Nuntawong, V. Patthanasettakul, A. Pokaipisit, and P. Limsuwan, "Dynamic in situ spectroscopic ellipsometric study in inhomogeneous TiO2 thin-film growth," J. Appl. Phys. **108**, 013522-1-013522-7 (2010).
25. E. Franke, C. L. Trimble, M. J. DeVries, J. A. Woollam, M. Schubert, and F. Frost, "Dielectric function of amorphous tantalum oxide from the far infrared to the deep ultraviolet spectral region measured by spectroscopic ellipsometry," J. Appl. Phys. **88**, 5166-5174 (2000).